

5-2016

Fabrication and Characterization of Heparin-Immobilized Electrospun Nanofibers for Vascular Suture Applications

Michael J. DiBalsi

Clemson University, mdibals@g.clemson.edu

Follow this and additional works at: https://tigerprints.clemson.edu/all_theses

Recommended Citation

DiBalsi, Michael J., "Fabrication and Characterization of Heparin-Immobilized Electrospun Nanofibers for Vascular Suture Applications" (2016). *All Theses*. 2336.

https://tigerprints.clemson.edu/all_theses/2336

This Thesis is brought to you for free and open access by the Theses at TigerPrints. It has been accepted for inclusion in All Theses by an authorized administrator of TigerPrints. For more information, please contact kokeefe@clemson.edu.

FABRICATION AND CHARACTERIZATION OF HEPARIN-IMMOBILIZED
ELECTROSPUN NANOFIBERS FOR VASCULAR
SUTURE APPLICATIONS

A Thesis
Presented to
the Graduate School of
Clemson University

In Partial Fulfillment
of the Requirements for the Degree
Master of Science
Bioengineering

by
Michael J. DiBalsi
May 2016

Accepted by:
Jeoung Soo Lee, Committee Chair
Robert Brown
Martine Laberge

Abstract

One of the most significant complications of vascular surgery is thrombosis, which is the formation of blood clots at the surgical site. Another significant complication is stenosis - an overgrowth of cells during the healing process, which narrows the same artery the surgeons were trying to open. These complications often lead to additional surgeries and carry increased morbidity and mortality for the patients. Numerous pharmaceutical agents have been tested to prevent these complications, but the results have been disappointing. The agents either have unacceptable systemic effects, or they cannot achieve a controlled, timed release in the circulation. Heparin is the most commonly used anti-coagulant for anastomotic thrombosis prevention, with numerous studies employing heparin-immobilized or heparin-coated biomaterials for improved thrombo-resistance.

In this study, the feasibility of heparin-immobilized electrospun nanofibers as surgical sutures was explored. Using a novel positively charged amphiphilic copolymer as well as PLGA and PEO, fibers were successfully prepared via electrospinning and twisted into uniform yarns. The yarns were characterized using FE-SEM and tensile testing. Fluorescein conjugated heparin was surface immobilized on the yarns through electrostatic interactions, and released out from the nanofibers. The therapeutic activity of the immobilized heparin was tested in vitro also. It was shown that the heparin loading efficiency was greatest in the yarn containing the highest weight percent of the positively charged PEI polymer and the release kinetics were more gradual and controlled compared

to control yarns. Further work needs to be done to improve the mechanical properties of the yarns to make them acceptable for commercial use.

Acknowledgements

I would like to thank my research advisor Dr. Jeoung Soo Lee for her assistance and guidance. I would also like to thank my committee: Dr. Martine LaBerge and Dr. Robert Brown for their time and patience. I also wish to thank my lab members Graham Temples, Christian Macks and Dr. So Jung Gwak for their help. In addition I would like to thank past and current lab members of the MicroEnvironmental Engineering Laboratory for teaching me necessary techniques and allowing me to use their lab space, especially Sooneon Bae who served as an excellent mentor, providing guidance and support throughout the course of my project. Additionally, I would like to thank Dr. Guzeliya Korneva for her assistance with electrospinning and Dr. Konstantin Kornev for his contributions to the electrospun yarn collection and preparation.

Table of Contents

	Page
TITLE PAGE	i
ABSTRACT.....	ii
ACKNOWLEDGMENTS	iv
LIST OF TABLES	vii
LIST OF FIGURES	viii
CHAPTER	
I. INTRODUCTION	1
1.1 Cardiovascular Complications	1
1.2 Free-Tissue Transfer	2
1.3 Vascular Anastomosis.....	2
1.4 Surgical Sutures	3
1.5 Electrospinning	4
1.6 Thrombosis & Stenosis.....	6
1.7 Heparin.....	7
II. CURRENT APPROACHES AND STATE OF KNOWLEDGE.....	9
2.1 Systemic Drug Administration	9
2.2 Localized Drug Administration	9
III. OBJECTIVES	13
3.1 Project Rationale & Aims	13
IV. MATERIALS AND METHODS.....	15
4.1 Materials	15
4.2 Synthesis of PgP	15
4.3 Electrospinning	17

Table of Contents (Continued)

	Page
4.3.1 General Setup.....	17
4.3.2 Polymer Solution Formation.....	17
4.3.3 Electrospinning.....	18
4.3.4 Fiber Collection and Yarn Formation.....	18
4.4 Physical and Mechanical Characterization Of Electrospun Yarns.....	19
4.4.1 Scanning Electron Microscopy.....	19
4.4.2 Phase Contrast Microscopy.....	19
4.4.3 Tensile Testing.....	20
4.5 Heparin Immobilization.....	21
4.5.1 Fluorescein Conjugation to Heparin.....	21
4.5.2 F-Heparin Surface Immobilization onto Electrospun Fibers.....	22
4.6 Heparin Quantitation.....	23
4.7 Heparin Release Study.....	23
4.8 Activated Partial Thromboplastin Time Study.....	24
 V. RESULTS AND DISCUSSION.....	 25
5.1 Synthesis and Characterization of PgP.....	25
5.2 Electrospinning.....	27
5.2.1 Polymer Selection.....	27
5.2.2 Polymer Concentration.....	28
5.2.3 Solvent Selection.....	28
5.2.4 Parameter Optimization.....	29
5.3 Electrospun Yarn Characterization.....	29
5.3.1 Physical Characterization.....	29
5.3.2 Mechanical Characterization.....	30
5.4 Heparin Loading and Release.....	33
5.5 Immobilized Heparin Therapeutic Activity.....	37
 VI. CONCLUSION AND FUTURE STUDIES.....	 38
6.1 Conclusion.....	38
6.2 Limitations and Future Studies.....	39
 REFERENCES.....	 40

List of Tables

Table		Page
1	Mechanical Properties of corresponding electrospun yarns	32
2	Yarn composition, PEI composition and heparin loading amount for each yarn type.....	34

List of Figures

Figure		Page
1	NMR spectrum of PgP1 and PgP 3.7	26
2	SEM images of electrospun yarns.....	30
3	Stress-strain plots of select PP PPP 1 and PPP 3.7 yarns	32
4	Heparin loading amount for each fiber	34
5	Fluorescent microscopy (10x magnification) of heparin-immobilized fibers	35
6	Release profiles of PP, PPP 1 & PPP 3.7 yarns	36
7	Clotting times of each type of heparin-immobilized yarn	37

Chapter 1

Introduction

1.1 Cardiovascular Complications

It is well documented that cardiovascular disease, defined as a class of diseases that involve the heart or blood vessels, is the leading cause of death in the United States, responsible for one of every four deaths annually [1]. There are numerous risk factors that contribute to cardiovascular disease, the most common including: high blood pressure, diabetes, high cholesterol, tobacco use, poor diet, physical inactivity, obesity, excessive alcohol consumption, and heredity. While the majority of cardiovascular problems can be avoided with personal lifestyle changes, surgical intervention is frequently required to mitigate the likelihood or prevent the occurrence of more serious conditions such as heart attack, stroke or amputation [2].

With the vast array of vascular procedures performed on a daily basis, the occurrence of resulting complications vary based on a myriad of variables such as the performance of the operating surgeon, the patient's individual biological response to the procedure, pre-existing health conditions in the patient prior to surgery, or the actual procedure performed. Nonetheless, even with all of the variables, two of the most common and significant complications associated with vascular procedures are thrombosis and stenosis [3], [4]. Thrombosis is the formation of a blood clot and can lead to vascular occlusion or emboli formation. Stenosis is the abnormal narrowing of a blood vessel, affecting proper blood circulation.

1.2 Free-Tissue Transfer

Moreover, these complications are not limited strictly to cardiovascular disease procedures. Free tissue transfer, a safe mode of tissue reconstruction, is utilized in a variety of surgical fields including oral maxillofacial, orthopedic, plastic and reconstructive, and otolaryngology. It involves the transplantation of tissue from one location (“donor site”) to the desired location (“recipient site”) and has multiple indications such as: skeletal defects after debridement for osteomyelitis, breast reconstruction, and various trunk and extremity defects. Composite tissue allotransplantation is also a newer form of free tissue transfer used primarily in the face and hand. For all free flap procedures, blood supply is reconstituted via microsurgical procedures to connect the vasculature from the native tissue to the graft. Despite meticulous technique and anti-coagulation drugs, there still exists a significant risk of thrombosis post-surgery. Thrombotic occlusion is the main cause of graft failure, with failure occurring in 4 percent of free flaps and up to 30 percent of digital replantations [5].

1.3 Vascular Anastomosis

In any procedure where vasculature is broken and requires either anastomoses or ligation, surgical sutures are predominantly used to connect or tie off the vessels. It is at this location where stenosis and thrombosis occur due to the disruption of the vascular endothelium, which activates the coagulation cascade and triggers a pro-inflammatory response [6]. In order to prevent these complications from occurring, it is imperative that

these mechanisms are limited or prevented entirely. Research has been done that either indirectly looks to treat the problem or focus on different complications associated with the application of surgical sutures.

1.4 Surgical Sutures

By definition, a suture is a natural or synthetic strand of textile that is used to ligate blood vessels and draw tissues together [7]. An ‘ideal’ suture should have adequate knot/straight strength, with appropriate strength and mass loss for its proposed usage. It should be pliable and easy to handle, sterile, biocompatible and uniform with predictable performance [8]. While no suture possesses all of these characteristics, it is left up to the clinician to select a suture that’s most appropriate for its intended use [9].

Sutures are classified as either absorbable or nonabsorbable, monofilament or multifilament, and consist of either naturally derived or synthetic materials. They are available in a wide range of sizes defined by the United States Pharmacopeia (USP). Absorbable sutures undergo chemical degradation in vivo, most commonly via hydrolysis. Sutures that lose a significant portion of their tensile strength within 2 months have been defined as absorbable, but now that current advances in materials have shown extended tensile retention times for six months or longer, it’s more of a loose definition [8].

Monofilament sutures are made of a single strand of material, exhibiting lower tissue drag compared to its multifilament counterpart. Multifilament sutures consist of multiple strands that are either braided or twisted together, affording greater tensile

strength, flexibility, and pliability [10]. The capillarity of multifilament sutures, which can serve as a nidus for bacteria, as well as its increased surface roughness can be overcome by coating the sutures, simultaneously enhancing the handling characteristics [8].

Suture manufacturing varies greatly depending on the material. Natural materials do not require extrusion for fiber formation, while synthetic materials do. Melt extrusion is the most common form, but gel spinning is sometimes necessary instead. After extrusion, the fiber is heated and oriented by drawing. This process aligns the molecular chains in the amorphous region to increase tensile strength along the fiber axis, as well as reducing fiber diameter. The braiding or twisting of multifilament fibers after orientation further stretches the fiber to tighten construction and form a single strand. Heat treatment, including annealing and/or relaxation, is then performed to relieve internal stresses associated with previous processing and increase dimensional stability. Finally, in some cases the suture strand is surface coated to impart various desired properties [8].

1.5 Electrospinning

Recently, an electrostatic fiber fabrication technique known as electrospinning has gained more interest and attention in the biomedical field. Electrospun nanofibers have high surface area to volume ratio, flexibility in surface functionalities, and mechanical properties superior to larger fibers [5]. Moreover, the prospect of large scale productions combined with simplicity in the process makes electrospinning engaging for a variety of

applications [11]. Specifically, their feasibility as wound dressings, drug delivery, and molecule immobilization has led to the exploration of their use as surgical sutures.

There are several setup configurations for electrospinning. The typical setup consists of three main components: a high voltage power supply, a spinneret (e.g. syringe needle) and a grounded collector. The nanofibers are fabricated by applying a high electrical charge to a droplet of a polymer solution, causing electrostatic repulsion that counteracts the surface tension and stretches the droplet. At a critical point a stream of liquid erupts from the surface forming a ‘Taylor cone’ which is a charged liquid jet that dries in flight on its way to the grounded collector. As a result of electrostatic repulsion, the jet is elongated and thinned in flight, forming uniform fibers with nanometer-scale diameters [12].

The polymer solution is composed of a dissolved polymer in a volatile solvent. A pump, which holds the syringe containing the polymer solution, regulates the rate at which the polymer solution is pumped out of the blunt tipped needle. The high voltage source consists of two electrodes, one from the positive power source, and one connected to a negative source, acting as the ground. The separation between the needle tip and the grounded mandrel, known as the gap distance, creates a static electric field [13].

Electrospinning in general is a very complex process due to the multitude of parameters that directly affect the process itself and the properties of the resulting fibers. These parameters can be classified into solution parameters, process parameters, and ambient parameters. Solution parameters include concentration, molecular weight of polymer, viscosity, surface tension, and conductivity/surface charge density. Processing

parameters include the applied voltage, feed rate/flow rate, collector type and tip to collector distance (gap distance). Ambient parameters include humidity, temperature, etc. [12].

1.6 Thrombosis & Stenosis

In order to address the problems of thrombosis and stenosis, it is important to fully understand what causes each and their respective mechanisms of action. Thrombosis is caused by one or more of three factors known as Virchow's triad: hypercoagulability, endothelial cell injury, and disturbed blood flow. Injury to the endothelium causes the exposure of the underlying collagen that causes platelets to bind and activate, triggering the coagulation cascade and ultimately leading to the formation of a fibrin clot. This is the chief factor associated with thrombosis caused by surgical intervention. The disturbance of blood flow is a secondary factor, as the hemodynamics will be affected by the presence of a suture as well as the resulting endothelial surface morphology of the anastomosed vessel.

Stenosis, the abnormal narrowing of blood vessels, is most commonly caused by atherosclerosis and characterized by intimal lesions that protrude into and obstruct vascular lumens and weaken the underlying media. The contemporary view of its pathogenesis is a chronic inflammatory response initiated by injury to the endothelium. The injury results in endothelial activation and dysfunction, yielding increased permeability and leukocyte adhesion. Monocytes then migrate into the intima where they transform into macrophages and foam cells. Release factors from activated platelets,

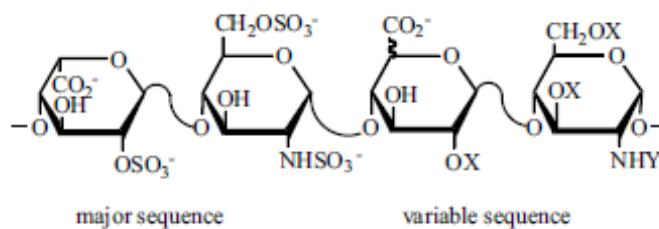
macrophages, or vascular cells cause the migration of smooth muscle cells from the media to the intima. Proliferation of VSMCs is highest in the first week after injury and can continue for 14–28 days depending on the severity of the injury [14]

1.7 Heparin

By understanding the pathology of thrombosis and stenosis as associated with vascular procedures, a focused approach can be taken to mitigate these complications. In the vascular surgery literature, the use of anticoagulation drugs has been shown to improve surgical outcomes and patency rates. Microvascular literature discusses the use of three main pharmacologic agents; heparin, aspirin, and dextran, as an adjunct to preventing thrombosis [4]. Heparin, a well-established anticoagulant, is the most commonly used agent for anastomotic thrombosis prevention, with numerous studies employing heparin-immobilized or coated biomaterials for improved thrombo-resistance. Specifically, immobilized heparin on biomedical devices is known to reduce platelet adhesion, increase plasma re-calcification time, and increase activated partial thromboplastin time (APTT) better than soluble heparin [15]. Moreover, it has been shown to have anti-proliferative effects on smooth muscle cells when administered in higher doses [16].

Heparin is a glycosaminoglycan containing a mixture of linear polysaccharides having 2-*O*-sulfo- α -L-iduronic acid, 2-deoxy-2-sulfamino-6-*O*-sulfo- α -D-glucose, β -D-glucuronic acid, 2-acetamido-2-deoxy- α -D-glucose, and α -L-iduronic acid as major

saccharide units joined through 1-4 glycosidic linkages. It's a relatively large polysaccharide, with its molecular weight ranging from 5,000-40,000. It has multiple chemically reactive functional groups, with each disaccharide repeating unit containing a carboxyl group. All repeating units have one or more 1° or 2° hydroxyl groups and approximately 2-2.5 sulfo groups. N-sulfo groups are present in 75-85% of all repeating units [15].



Scheme 1. General Structure of Heparin; X=H or SO_3 ; Y=Ac or SO_3

Chapter 2

Current Approaches and State of Knowledge

2.1 Systemic Drug Administration

The majority of treatments currently used to combat thrombosis and stenosis involve the use of drugs delivered systemically. This approach has been generally disappointing, with the agents producing unacceptable systemic effects or their inability to achieve a controlled and sustained release in circulation. A study performed in 2006 by Chung et. al investigating a combinatorial approach of tirofiban, aspirin, and heparin for the prevention of microsurgical anastomotic thrombosis in a thrombogenic rat model showed a significant increase in arterial and venous patency and decrease in thrombus formation. However, these agents were administered intravenously during surgery [4].

2.2 Localized Drug Administration

With the increasing application of electrospun nanofibers as drug delivery systems, multiple studies have explored the feasibility of incorporating heparin into the fibers. In 2006, Luong-Van et al. loaded heparin onto the surface of poly(ϵ -caprolactone) electrospun mats and achieved a sustained, diffusionally-controlled release of heparin over 14 days with no pro-inflammatory response in vitro [14]. A very similar study was done in 2009 by Su et al. that encapsulated heparin into electrospun poly(L-lactide-co- ϵ -caprolactone) fiber mats via co-axial electrospinning and investigated their effect on VSMC proliferation in vitro over a seven day period [17].

It wasn't until around a decade ago that the notion of incorporating drugs within or onto the surface of sutures began to be investigated. This approach allows for a localized delivery of therapeutic agents while avoiding excessive systemic levels, thus improving the therapeutic index. Moreover, since sutures are already used in essentially all surgical procedures, drug-eluting sutures would reduce the amount of objects needed in the surgical bed. This could reduce the chances of infection, create more space on the sterile tool table, and eliminate the need for additional materials or therapeutics to be applied to the sutured area.

In a study published in 2008, He et al. successfully fabricated two kinds of drug-loaded fibers using blend and coaxial electrospinning techniques. The aligned drug-loaded fiber bundles were then further processed into fibrous threads by twisting and hot-stretching treatments. The drug used was TCH, a broad-spectrum antibiotic, and PLLA was the polymer used. In vitro drug release studies showed that the coaxially-spun threads suppressed an initial burst release while providing a sustained release pattern, while the blend-spun threads produced a large initial burst release. Although the tensile strength of the fabricated threads were lower than current commercially used sutures, the authors believe that their study showed a promising method to develop drug loaded sutures [18].

A few years later, Hu et al. ran a very similar study, where they combined a braiding technique with the electrospinning process. The drug that was used was cefotaxime sodium, a broad spectrum third-generation antibiotic. Moreover, the fibers were coated with chitosan, due to its favorable blood compatibility and hemostasis

behavior. The polymer of choice (PLLA) for electrospinning was the same as He et al.'s study as well as their characterization method with the results yielding preferable morphology and tensile properties as well as favorable antibacterial performance. An in vivo study was also performed on rats to test for biocompatibility, yielding mild tissue reactions as compared with two commercial sutures [19].

In 2012, Weldon et al. published a study exploring biodegradable drug-eluting electrospun sutures for local anesthesia. The sutures were composed of PLGA, an FDA approved biodegradable polymer used in commercially available sutures, and bupivacaine hydrochloride, a commonly used amino-amide local anesthetic. The fiber bundles created were equivalent to 6-0 (~0.08 mm diameter), 4-0 (~0.175 mm), and 2-0 (~0.32 mm) suture gauge sizes. Their results demonstrated similar tissue reaction in vivo to commercially available sutures as well as adequate mechanical properties for proper wound healing. The entire drug was released from the suture within 12 days and maintained approximately 12% of their initial tensile strength after 14 days of incubation in vitro. The tensile strength of the electrospun sutures was also decreased as the drug concentration increased, but the strains remained relatively similar from group to group [20].

In 2013, Lee et al. had a study published in *Acta Materialia* using a slightly different approach to drug-loaded sutures. Concerned with the commonly observed adverse mechanical strength effects of the preparation methods proposed for drug-releasing sutures, their team looked to simply coat commercially used sutures with drug-loaded electrospun sheets. PLGA and ibuprofen were electrospun together and then

braided by hand around the surface of the surgical suture. In vitro release studies and in vivo animal (rat) pain evaluation studies were conducted as well as the common mechanical properties tests. Based on their results, they concluded that their suggested approach is a novel system for postoperative pain relief and that their fabrication method will allow for numerous different drugs to be used in the future [21].

The most recent study found that also is the most similar to the proposed research plan in this paper. Dexamethasone (DEX), a glucocorticoid that inhibits inflammatory processes and proliferation of SMCs, was loaded into PLGA particles using a water-oil emulsion method. Next, the surface of the particles were treated to enhance their hydrophilicity and then dispersed in polyethyleneimine (PEI). These PEI-coated particles were then dispersed in distilled water and a commercially used absorbable suture (4-0 Vicryl) was immersed in the suspension. The positively charged surface of the modified particles allowed for them to be immobilized onto the suture via electrostatic interactions. The particles were found to remain on the suture surface after 4 weeks in PBS at 37°C with a sustained DEX release over the 4-week incubation period. Moreover, the presence of the immobilized particles did not affect the mechanical properties of the absorbable sutures [22].

Chapter 3

Objectives

3.1 Project Rationale & Aims

The goal of this proposed research is to develop a drug-eluting suture incorporating a novel, cationic, amphiphilic block copolymer, polyethylenimine-g-poly (D, L-lactide-co-glycolide) (PgP), which we have synthesized in our lab. To create this suture, we will use electrospinning, a simple and versatile method for developing polymeric fibers with very small diameters [14], [18], [19], [23], [24].

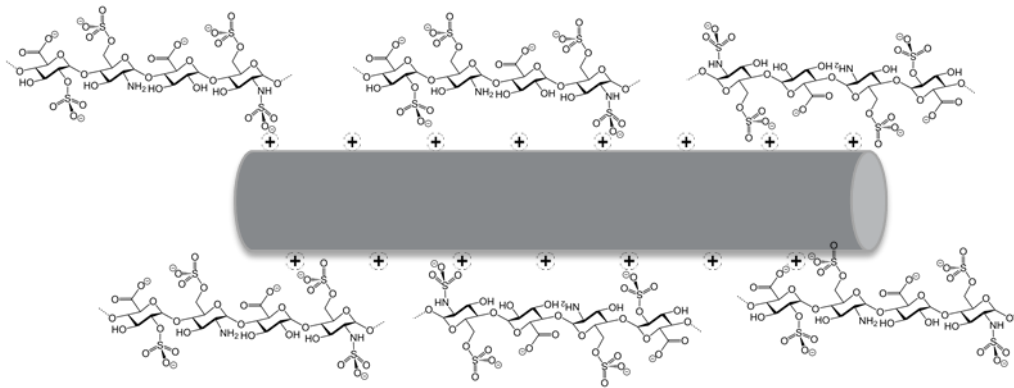
Once the polymer solution is electrospun into nanofibers, the fibers will be physically twisted together, forming a uniform yarn. It is hypothesized that heparin, a negatively-charged anti-thrombotic drug, will bind to the surface of the positively-charged, hydrophilic block of the PgP polymer (scheme 2). The electrostatic binding between the fiber and heparin molecules will allow for a sustained release of heparin to aid in the prevention of thrombosis and stenosis. This localized delivery of heparin to the site of anastomosis will reduce the amount of heparin that would normally be administered systemically, therefore yielding low systemic effects and reducing the amount of prophylactic treatments used in typical vascular procedures. Heparin was selected as therapeutic because of its widely recognized success in biomedical devices as well as its highly negative charge density that allows it to bind to the positively charged PEI.

Specifically, the aims of this study are as follows:

Aim 1: Fabricate and characterize the mechanical properties of heparin-loaded electrospun fibers

Aim 2: Evaluate the loading efficiency and release kinetics of immobilized heparin from the electrospun yarns

Aim 3: Evaluate the therapeutic activity of released heparin from the electrospun yarn



Scheme 2. Heparin loaded electrospun fiber

Chapter 4

Materials and Methods

4.1 Materials

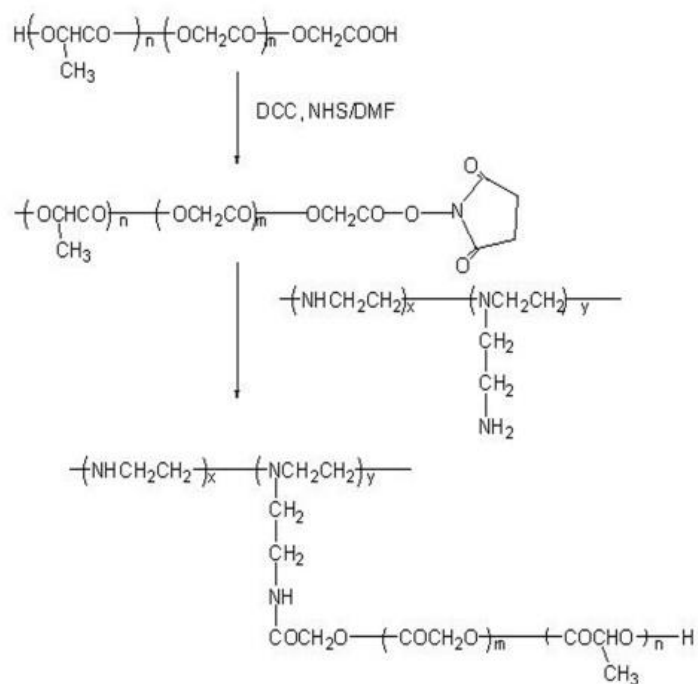
Poly (lactic-co-glycolic acid) (PLGA) (50:50, 50 kDa; 50:50, 100kDa) was purchased from Durect Corporation (Cupertino, CA). Heparin sodium salt from porcine intestinal mucosa, poly(ethylene oxide) (PEO) (1,000 kDa), anhydrous dimethylformamide (DMF), N,N-Dimethylacetamide (DMAc), N-hydroxysuccinimide (NHS), dicyclocarbodiimide (DCC) and branched polyethylenimine (b-PEI) (25kDa) were obtained from Sigma-Aldrich (St. Louis, MO). Dialysis tubing (MWCO: 50kDa, 300kDa) was obtained from Spectrum labs (Rancho Dominguez, CA). Dimethyl sulfoxide (DMSO) was obtained from Thermo Fisher Scientific (Waltham, MA). Disposable PD-10 Desalting Columns were obtained from GE lifesciences (Pittsburg, PA). 4'-(aminomethyl)fluorescein, hydrochloride was obtained from Molecular Probes (Eugene, OR).

4.2 Synthesis of polyethylenimine-g-poly (D, L-lactide-co-glycolide) (PgP)

PgP synthesis was carried out using two different molar ratios of PLGA:PEI (1.2:1 and 10:1 mole ratio). After adding a molecular sieve to DMF overnight to remove residual water, PLGA (50kDa) was dissolved in the solvent. NHS and DCC was then added to the reaction solution and stirred at room temperature for 2 hours to activate the carboxylic acid end group of PLGA. The resulting precipitate, dicyclohexyl urea (DCU) was filtered using a fine pore size glass funnel. Branched PEI (25kDa) was dissolved in

dried DMF and added in drop-wise fashion to the activated PLGA filtrate for 30 minutes. The mixture was allowed to react for 24 hours at room temperature with stirring.

The reaction solution was then pipetted in dialysis membranes (MWCO=50,000) and dialyzed against deionized water for two days, changing the water at 2, 4, 6, and 24 hour timepoints. The dialyzed product was then centrifuged for 10 minutes at 5,000rpm, forming a precipitate and supernatant which were separated and lyophilized. After synthesis and purification, the structure of the PgP was verified by ¹H- NMR on a Bruker 300MHz in deuterated DMSO (DMSO-d₆).

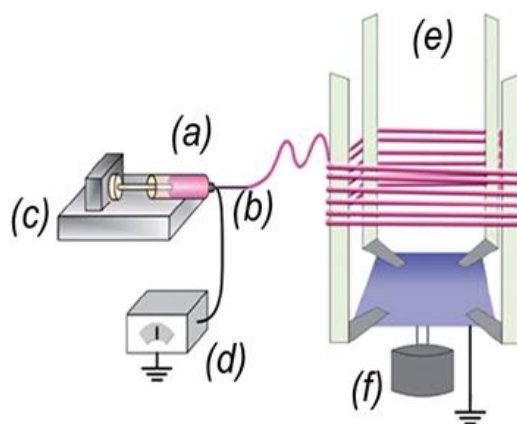


Scheme 3. Synthesis of PLGA-g-PEI

4.3 Electrospinning

4.3.1 General Setup

The electrospinning setup used for this study was designed by Dr. Kornev's group [25] and consisted of a syringe pump (c) elevated on an adjustable platform, a high voltage power supply (d), a grounded rotating mandrel collector (e), a charged polymer solution (b) and a syringe with a blunt tipped needle (a) from which the polymer is expelled (scheme 3). A heat sleeve was placed around the syringe (not shown) to keep the polymer heated during the electrospinning process.



Scheme 4. Illustration of electrospinning apparatus for fabricating and collecting nanofibers

4.3.2. Polymer Solution Formation

PLGA (50:50, 100 kDa) was warmed to room temperature (RT) then added to dimethylacetamide (DMAc) in a glass vial. The solution was capped and stirred with a stir bar on a stir plate at RT until fully dissolved. PEO (1,000 kDa) was then added and stirred further with heat ($\sim 60^{\circ}\text{C}$) until fully dissolved. Depending on the type of fiber being spun, Pgp was then added and stirred with heat until fully dissolved.

4.3.3 Electrospinning

Once the polymer was fully dissolved in the solvent, it was added to the syringe tube, being sure to remove any bubbles between the needle tip and the plunger. The syringe was then wrapped in the heat sleeve and placed in the syringe pump setup. The flowrate and inner diameter of the syringe tube was set on the pump, and pumping was started immediately to ensure the polymer didn't solidify in the needle. The positive electrode was clipped to the needle tip and the negative electrode was configured as a brush that made constant contact with the rotating mandrel. The applied voltage, relative humidity, gap distance, polymer solution flowrate, mandrel rotation speed and spinning time were all recorded for each spin. After optimal parameters were determined (through literature review and trial and error) the controllable parameters were held constant from batch to batch.

4.3.4 Fiber collection and Yarn Formation

To collect the aligned fibers from the mandrel and twist them into uniform yarns, a custom made collecting device was used (scheme 4). The brush-like ends were adjusted to the inner distance between two of the mandrel bars. Beginning at the bottom of the mandrel, the device was slowly raised between the bars while manual spinning the brushes to collect the fibers, resulting in a cylinder-like web once completed. After fibers were collected from one of the sides, the collector was placed in its mount, plugged in, and turned on, causing the brushes to spin in opposite directions and twisting the attached fibers into a tight, uniform yarn. The twisting time was noted for each batch and held constant once an optimal time was found for a given fiber. After twisting, the ends of the

yarn still connected to the brushes was cut with scissors and stored in petri dishes in a desiccator until further use.



Scheme 5. Custom-made fiber collector and twisting device

4.4 Physical and Mechanical Characterization of Electrospun Yarns

Following fabrication of the yarns, their physical and mechanical properties were characterized.

4.4.1 Scanning Electron Microscopy

Field Emission Scanning Electron Microscopy (FESEM) was used to observe the yarns' surface morphologies as well as the individual fibers' morphology. Samples were fixed to a SEM stage using double sided tape and sputter coated with palladium/platinum for approximately 60 seconds. Using an S-4800 SEM (Hitachi), images were taken at 150x and 1000x magnification with a 12.0kV accelerating voltage applied.

4.4.2 Phase Contrast Microscopy

Phase contrast microscopy (Zeiss Axiovert 200) was used to accurately measure the diameters of the yarns and observe their uniformity. Three images of each yarn were taken (from the center portion and the two ends) under 10x magnification. Three

measurements were then made from each of the three images and the resulting average diameter was used in calculating the yarns' tensile properties.

4.4.3 Tensile Testing

In order to characterize the mechanical properties for the various yarns that were electrospun, a MTS Synergie 100 (MTS Systems Corp.) material testing machine was used to perform tensile tests on the samples. The machine was connected to a computer that used the corresponding software (TestWorks® 4) to analyze the data. The yarns were cut into 5cm segments and clamped into the platents (grips), which were lined with Gator P100 sandpaper (Ali Industries, Inc.) to prevent slippage. After the given yarn sample was securely clamped into the platents, the top platent was raised to the point where the sample was taught but not stressed. The gauge length (distance between platents) was measured and input into the software, which was maintained as close to 30cm as possible for consistency. The average diameter of the given sample (measured as described previously via phase contrast microscopy) was also input into the program prior to running the test. Using a 100N load cell, the samples were evaluated under uni-axial tension at a constant rate of 5.0 mm/minute. Tests were run until failure, at which point the machine was stopped manually.

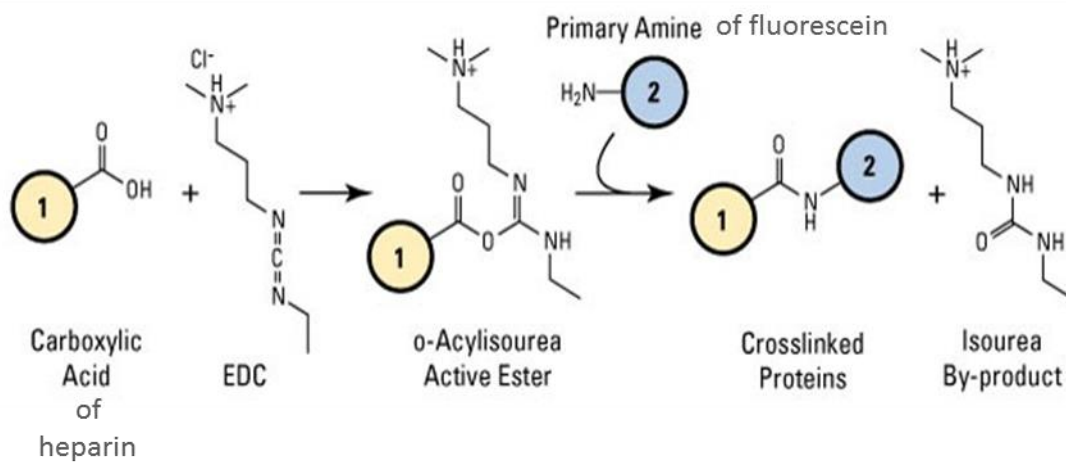
The software provided load, extension, stress and strain values, as well as peak load, peak stress, strain at break, and elastic modulus values for each sample. However, the automated moduli calculations were oftentimes not completely accurate based on observation of user-created stress-strain plots, so they were manually calculated. This

was accomplished by selecting two points at random in the linear elastic region of the plot and finding the slope of imaginary line between them.

4.5 Heparin Immobilization

4.5.1 Fluorescein Conjugation to Heparin

In order to visualize and quantify the amount of heparin that was immobilized to the electrospun fibers, a fluorophore was covalently bonded to it. Using a method modified from Osmond et al. [26], a 10% N-(3-dimethylaminopropyl)-N'-ethylcarbodiimide hydrochloride (EDC) solution was prepared in 0.1 M 4-morpholinoethanesulfonic acid (MES) buffer (pH 4.7). This solution was added to a 1% heparin solution in MES buffer, activating the carboxylic acid groups of heparin. Next, a 16% 4'-(aminomethyl) fluorescein hydrochloride solution was prepared in dimethylformamide (DMF) and added to the activated heparin solution, resulting in a covalent amide bond between the primary amine of the fluorescein and the activated carboxyl group of the heparin. The reaction mixture was sealed, protected from light and stirred at room temperature overnight. The fluorescein conjugated heparin (F-heparin) was purified using disposable PD-10 desalting columns with filtered deionized water and lyophilized to yield a powdered product.



Scheme 6. F-heparin conjugation reaction. Adapted from ThermoFisher [27]

4.5.2 F-Heparin Surface Immobilization onto Electrospun Fibers

Pre-weighed electrospun yarns were measured for length, washed 2x in deionized water and added to individual wells of a 24 well plate. 1 mL of 0.1% F-heparin solution in PBS (without Ca^{2+} and Mg^{2+}) was added to half of the samples, while plain PBS was added to the other half as negative controls. The yarns were protected from light and incubated at room temperature for 4 hours with gentle shaking. They then were briefly washed 2 times each with fresh PBS to remove any unbound f-heparin, dried with a kimwipe and lyophilized.

4.6 Heparin Quantitation

After lyophilization, the yarns were weighed and their diameters were measured again to see if any significant changes in weight or morphology had occurred. Next, the yarns were fluorescently imaged using an AMG EVOS FL cell imaging system to visualize the f-heparin loading efficiency. To quantify the amount of f-heparin loaded, the yarns were added to 200 μ L of PBS in individual wells of a black 96 well plate and their fluorescence was read using a Biotek Synergy4 multi-detection plate reader. F-heparin/PBS standards were also generated and read on the same well plate as the fibers. The standard curve was applied to the sample readings and the results were standardized by dividing the amount of F-heparin loaded by each sample's respective post heparin-immobilization and lyophilization weight. The negative control readings were averaged and then subtracted from their corresponding samples to eliminate the noise caused by the fiber itself.

4.7 Heparin Release Study

F-heparin immobilized yarns were placed in individual wells of a 24 well plate and 1mL of pre-warmed 37°C PBS was added to each well. The plate was protected from light and incubated at 37°C to mimic physiological conditions. At designated time points, 500 μ L of PBS was removed from each well and replaced with 500 μ L of fresh PBS. The PBS that was removed from the release plate was pipetted into a black 96 well plate (200 μ L each well, 2 wells per sample) and read by a microplate reader to measure its

fluorescence (Excitation: 494nm Emission: 521nm). A standard curve of f-heparin/PBS was used to quantify the readings.

4.8 Activated Partial Thromboplastin Time Study

To observe the activity of the immobilized heparin on the yarns, a timed clotting test was performed. 400 μ L of 1x PBS (without Ca²⁺ and Mg²⁺) was added to each well of a sterile 24 well plate. A pre-weighed yarn sample (~0.5mg) or 10 μ L of either a heparin/PBS standard or PBS were added to the wells. 500 μ L of pre-warmed (37°C) bovine platelet rich plasma (PRP) was then added to each well and the plate was shaken gently for 5 minutes at room temperature. Following shaking, the plate was incubated for 20 minutes at 37°C to mimic physiological conditions. 0.1M calcium chloride (CaCl₂) was prepared in filtered deionized water and warmed to 37°C in a water bath. 100 μ L of the CaCl₂ was added to each well to activate the coagulation cascade, and the time it took for each well to form a clot was recorded. A clot was observed when the clear solution started to become cloudy, eventually leading to a gel-like phase. The assay was run twice with 3 of each sample tested per run. The average times were taken and compared against control wells.

Chapter 5

Results and Discussion

5.1 Synthesis and Characterization of PgP

PgP was synthesized using branched polyethylenimine (bPEI or PEI, MW 25kDa) and poly-D,L-(lactide-co-glycolide) (PLGA, MW 50kDa (50:50 lactide:glycolide)) To test the effect of the amount of hydrophobic polymer has on the composition ratio of PLGA:PEO:PgP, heparin loading efficiency and mechanical strength, two different PgPs were synthesized using two different mole ratios of PLGA to PEI (PLGA:bPEI=1.2 :1 and 10:1). Following synthesis and purification, the structure and grafting ratio of PLGA to bPEI were confirmed by ¹H-NMR (Bruker 300MHz) using DMSO-d₆ as a solvent. (δ =2.4~3.5 (m, PEI backbone -CH₂), δ =1.4~1.6 (d, 3H, PLGA -CH₃), δ =4.3 (q, 1H, PLGA-CH), δ =3.9 (s, 2H, PLGA -CH₂)). In case of PgP1, the ratio of the integrals of the PEI backbone (δ =2.4~3.5) to the methylene of PLGA (δ =3.9) indicated that approximately 1 PLGA (MW: 50 kDa) was grafted to each bPEI (figure 1A). In case of PgP 3.7, 3.7 of PLGA was grafted to each bPEI (figure 1B).

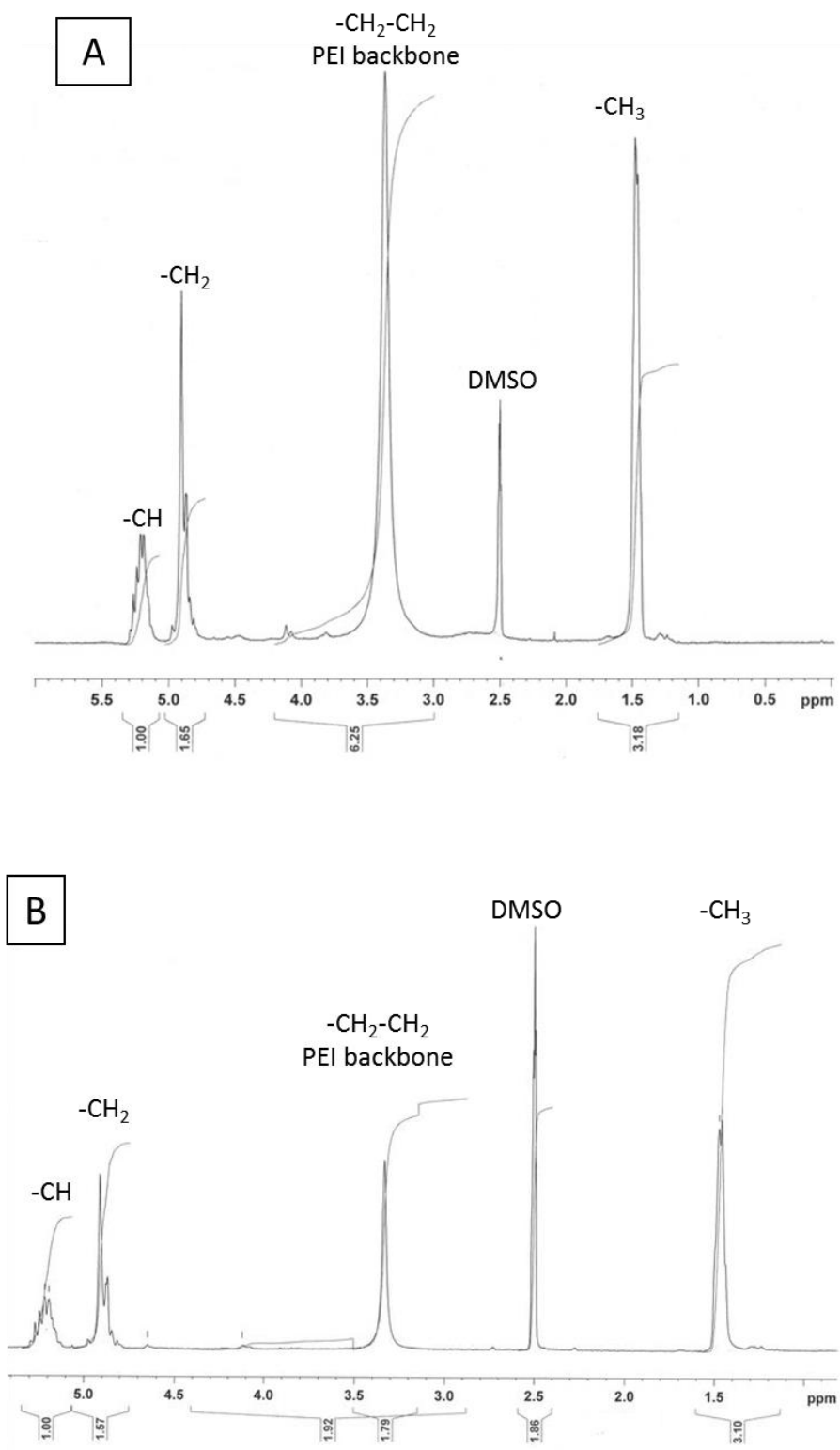


Figure 1. NMR spectrum of PgP1 (A) and PgP 3.7 (B)

5.2 Electrospinning

As previously described, there are a number of factors that influence the spinability, fiber morphology and mechanical properties of the resulting fibers.

5.2.1 Polymer selection

The polymers that were selected to be electrospun were chosen based on several factors. PLGA is FDA approved for use in humans and is one of the polymers used in common commercially available sutures [28]. It can also be dissolved in a wide range of common solvents [29], which aids in its ability to be electrospun [12]. The choice of high molecular weight PLGA was based on several reasons. First, since molecular weight is correlated with solution viscosity, the increased viscosity allows for continuous fiber formation as well as more uniform fiber diameter [12]. The high molecular weight is also shown to decrease degradation rates [30], an important characteristic in absorbable sutures.

Poly(ethylene oxide) (PEO), an amphiphilic polyether diol, is non-toxic and can be eliminated via hepatic and renal pathways. It was selected due to its ability to facilitate electrospinning of other polymers that are unable to be spun and improve the fiber's properties [31][32]. Although PEO is highly soluble in water, potentially negatively impacting the mechanical strength of the overall yarn, it has been shown that nanofibers fabricated with around 10wt% experienced no significant change in morphology and its fibrous structure was retained after 7 days immersed in water [33]. PEO's swelling properties in water allow for the void created by the suture needle to be filled, which is particularly useful in cardiovascular applications where minimal leakage at anastomosis

sites is desired [8]. Moreover, based on preliminary experiments, PgP could not be electrospun with PLGA alone; it wasn't until the addition of 2w/v% was added to the polymer solution. Furthermore, other preliminary studies of the effect of heparin immobilization and lyophilization on the yarns mechanical properties showed similar rates of reduced strength from pure PLGA yarns compared to PLGA/PEO and PLGA/PEO/PgP yarns.

5.2.2 Polymer Concentration

The concentration of each polymer used was determined by both literature review and experimentation. As described above, the low PEO concentration (2% w/v) allowed for PgP to be electrospun in the blend while avoiding extreme mechanical and morphological degradation in vivo [33]. PLGA has been electrospun in a number of studies at various concentrations, frequently between 10-20% w/v [34][35][36][37]. Through preliminary testing and mechanical testing, it was determined that 13% PLGA provided the most favorable fiber properties. PgP concentration was determined simply by its maximum solubility in the polymer solution blend. By increasing the ratio of PLGA:PEI in the PgP polymer, more PgP was able to be dissolved in the blend, ultimately allowing for a higher concentration of PEI electrospun into the fibers.

5.2.3 Solvent selection

The choice of solvent for the polymer solution has a big influence on its spinability, since most importantly it must be able to dissolve the polymer blend completely while maintaining the integrity of the polymer itself. Since PgP has shown poor solubility in many solvents commonly used for electrospinning, preliminary studies

were carried out to determine a suitable solvent. Through trial and error, it was determined dimethylacetamide (DMAc) was able to produce continuous, uniform fibers. However, in order to dissolve all 3 polymers and maintain an appropriate viscosity for electrospinning, the solution had to be heated to 60°C and maintained throughout the electrospinning process. This was achieved by wrapping the electrospinning syringe in a heat sleeve.

5.2.4 Parameter Optimization

As stated in the background section on electrospinning, there are a multitude of variables that affect the electrospun fiber spinnability and morphology [13]. The applied voltage, gap distance, polymer flow rate, needle gauge, relative humidity, all must be optimized and then remain consistent for repeatability. However, based on the polymer solution being electrospun, they were adjusted slightly for best results the gap distance was set between 20-25cm, needle gauge was 21, polymer flow rate was 0.25mL/hr, applied voltage was +12kV -2kV, and relative humidity was between 40-60%. The twisting of the fibers into yarns has also been shown to improve mechanical strength of the yarn [38].

5.3 Electrospun Yarn Characterization

5.3.1 Physical Characterization

The scanning electron microscopy (SEM) images (figure 2) show the surface morphology of the electrospun fibers produced with and without PgP. The relatively smooth surface of the yarns and the uniform nanofiber diameter are both favorable

properties for suture design and mechanical strength, respectively. It can also be observed that the fibers are uniformly oriented, which has been shown to improved mechanical strength of the yarn [13][39][40].

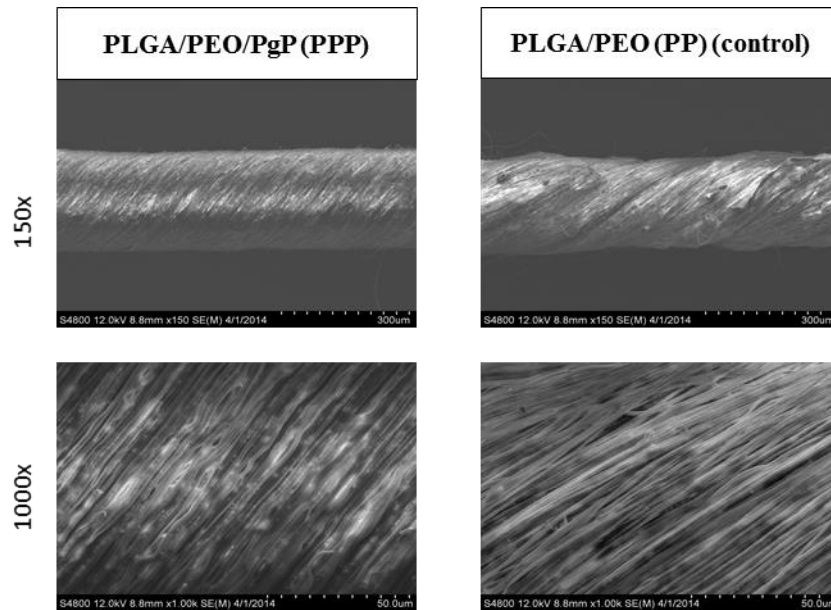


Figure 2. SEM images of electrospun yarns

5.3.2 Mechanical Characterization

The mechanical properties of the yarns are given below. The fiber diameter's were approximated to USP 6-0 size, slightly larger than sutures typically used for microvascular anastomosis but still small enough for vascular applications elsewhere in the body [41]. While the only standard requirement set forth by the United States Pharmacopeia (USP) is a suture's minimum knot-pull tensile strength [8], the elastic modulus and elongation at break values provide insight into the overall mechanical behavior of the yarns and are frequently provided in similar literature [28][8][19][9][22][35].

As seen in the stress-strain plots (figure 3), the yarns containing the PgP show a much larger elongation at break value than the non-PgP yarns. Apart from this however, there was only a significant difference in the elastic moduli between the PgP and non-PgP fibers which is a good measure of the material's stiffness. It must be noted, however, that the mechanical strength displayed in the yarns are well below the standards for comparable absorbable sutures of similar diameters. While the tensile strength of the yarns in this study were around 15 MPa, sutures of similar size require strengths approximately 20x higher as provided by the USP.

Comparable commercially available sutures like Ethicon's Vicryl® suture, which is an absorbable multifilament suture composed of PLGA, has a minimum ultimate strength of 410 MPa and a minimum elastic modulus of 1.4 GPa [8]. Moreover, studies were done on the mechanical strength of the yarns after heparin immobilization and lyophilization as well as seven days after incubation in PBS at 37°C which showed significant decreases in mechanical strengths. These significant discrepancies between the electrospun yarns and the commercial suture consisting of similar polymers show how PLGA itself isn't the problem but that the various other parameters all contribute to the final product's mechanical properties.

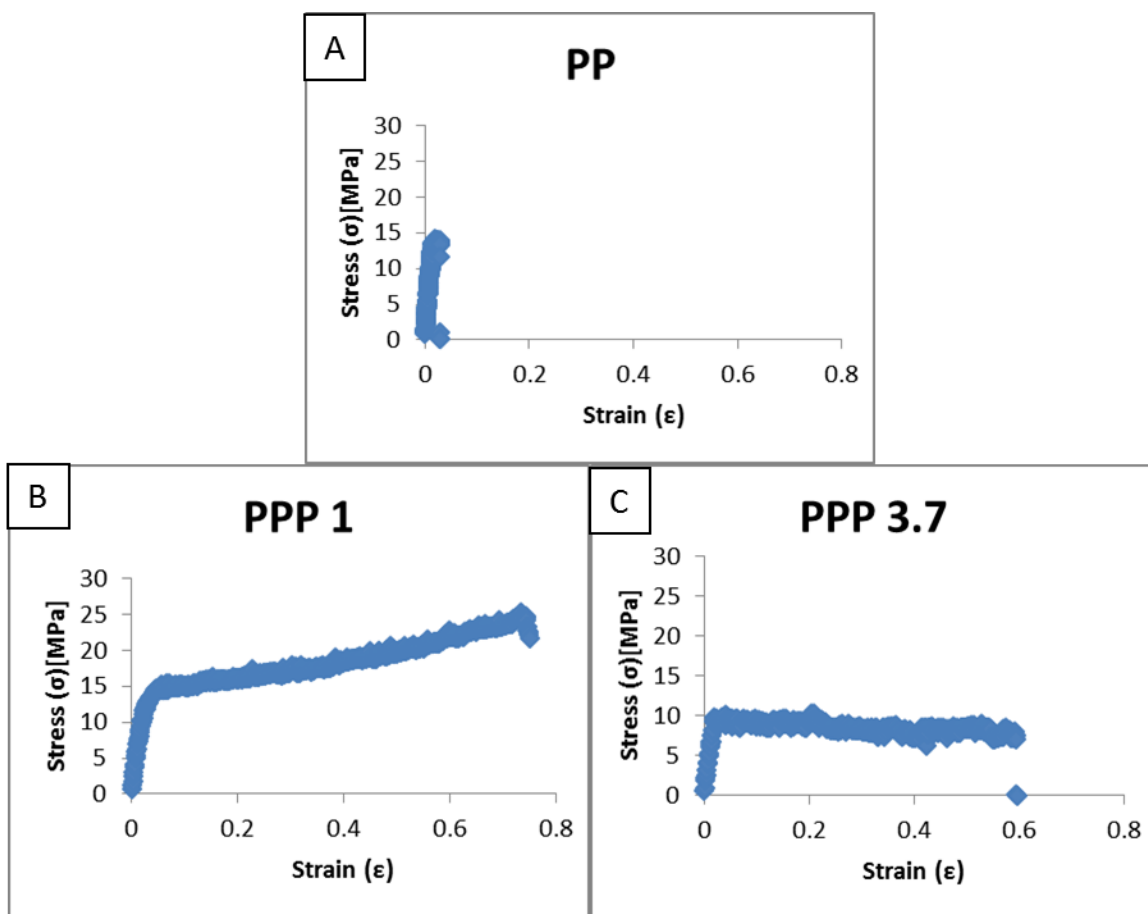


Figure 3. Stress-strain plots of select PP (A) PPP 1 (B) and PPP 3.7 (C) yarns

Table 1. Mechanical Properties of corresponding electrospun yarns

Fiber Type	Fiber Diameter [μm]	Elastic Modulus [MPa]	Elongation at Break (%)	Tensile Strength [MPa]
PPP 3.7	92.74 \pm 20.11	453.25 \pm 31.95	67.2 \pm 18.4	13.4 \pm 4.37
PPP 1	105.56 \pm 18.67	487.55 \pm 31.82	78.44 \pm 5.71	23.34 \pm 4.97
PP	93.00 \pm 5.93	666.99 \pm 52.85	2.90 \pm 1.48	10.93 \pm 3.07

5.4 Heparin Loading and Release

Heparin was surface immobilized for several reasons. The possibility of the heparin being denatured due to the solvent (DMAc) or the high voltage necessary for electrospinning is avoided, while the high surface to volume ratio of the nanofibers is able to be used to load high concentrations of heparin. More importantly, preliminary studies testing the feasibility of incorporating heparin in the polymer blend prior to electrospinning produced fibers with very poor mechanical properties. While it was observed that mechanical properties decreased after heparin surface immobilization, they were still far superior to the heparin blended fibers.

By surface immobilizing heparin post-electrospinning, the ionic bonding between the negatively charged sulfate groups on heparin and the positively charged amine groups on the PEI allow for these electrostatic interactions to bind more heparin per mg fiber (figure 4). As expected, the increase in the total amount of PEI present in each yarn resulted in an increased amount of immobilized heparin. The presence of immobilized heparin on the PP fiber is due to hydrophobic interactions, which are weaker than electrostatic but still exhibit some level of attraction. The heparin loading was also shown visually via fluorescent microscopy (figure 5). While the discrepancies between images is hard to observe, it is import to note that the difference in heparin loading between each yarn is on the microgram level.

Table 2. Yarn composition, PEI composition and heparin loading amount for each yarn type

Fiber Type	Fiber Composition (Weight Ratio, w/v %)	PEI Amount [w/v %]	Heparin Loading [$\mu\text{g}/\text{mg}$ fiber]
PPP 3.7	PLGA:PEO:P _{3.7} gP (13.0:2.0:1.5)	0.179	3.21 \pm 0.12
PPP 1	PLGA:PEO:PgP (13.0:2.0:0.39)	0.132	1.63 \pm 0.21
PP	PLGA:PEO (13.0:2.0)	0	1.03 \pm 0.06

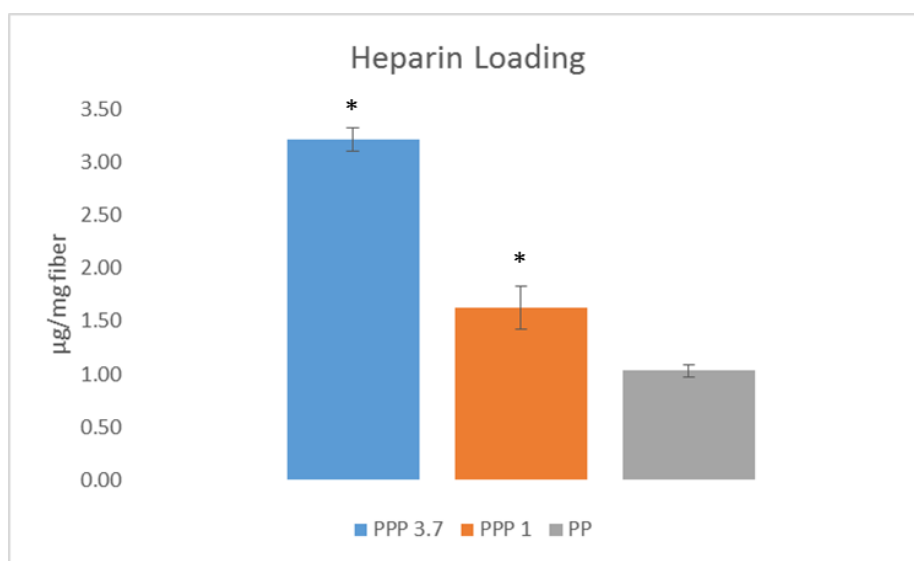


Figure 4. Heparin loading amount for each fiber. * $p < 0.05$ compared to PP fiber

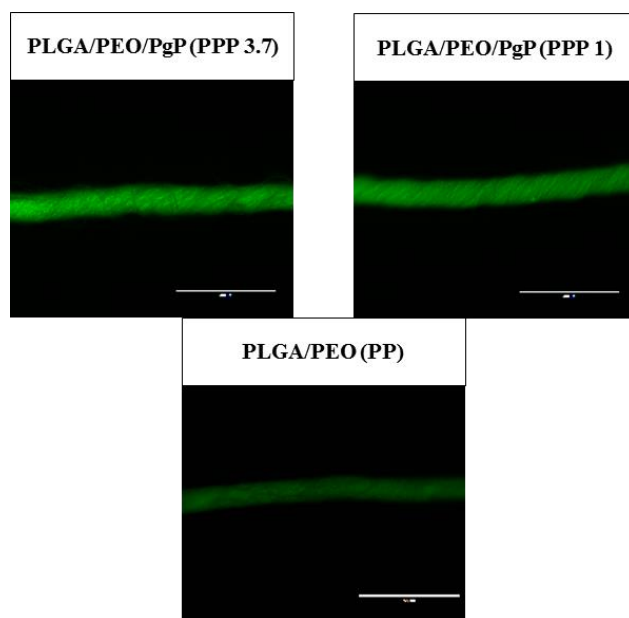


Figure 5. Fluorescent microscopy (10x magnification) of heparin-immobilized fibers

The release profile of heparin from the yarns over a 20 day period can be seen below (figure 6A). The electrostatic effect is observed again through the slightly slower rate of release over the first few days. While all 3 yarns displayed burst release, there were significant differences between each fiber, especially over the first 8 hours (figure 6B). The PP yarn had released over 70% of the heparin that was immobilized, while the PPP 1 yarn only released around 50% and the PPP 3.7 yarn slightly over 25%. This initial burst release is a favorable characteristic since bolus injections of heparin are commonly applied to the wound area during surgery anyway. It has been shown that immediate heparin treatment is more effective than delayed administration for preventing the myoproliferative response [42]. Vascular smooth muscle cell (VSMC) proliferation is highest in the first week of injury, and heparin release was sustained well past this point [14].

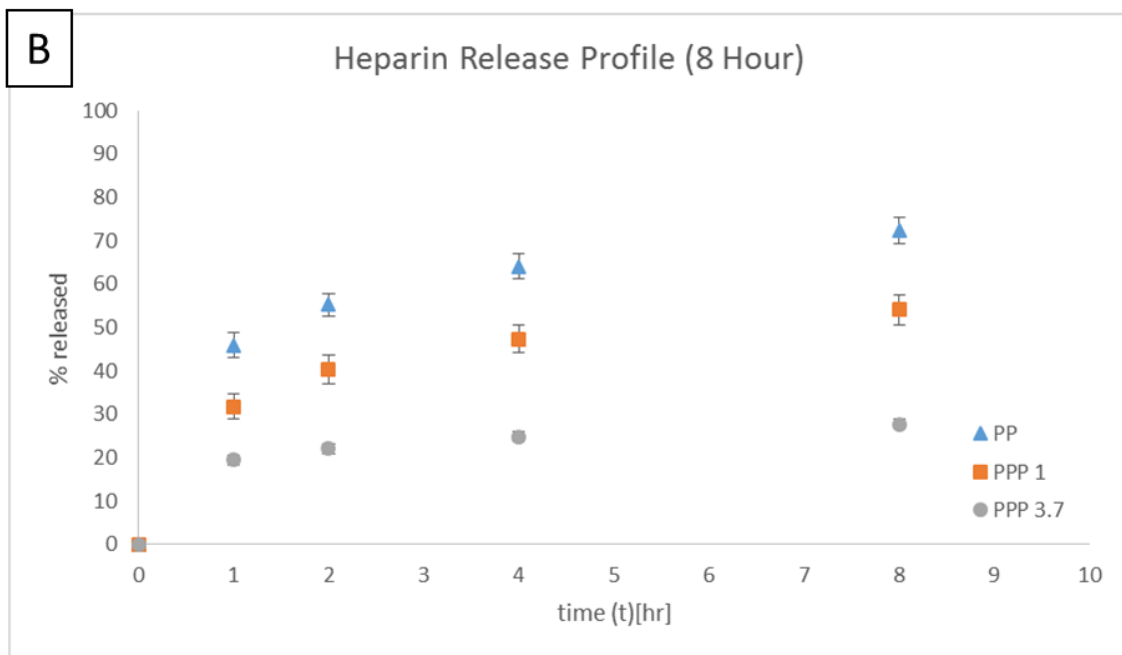
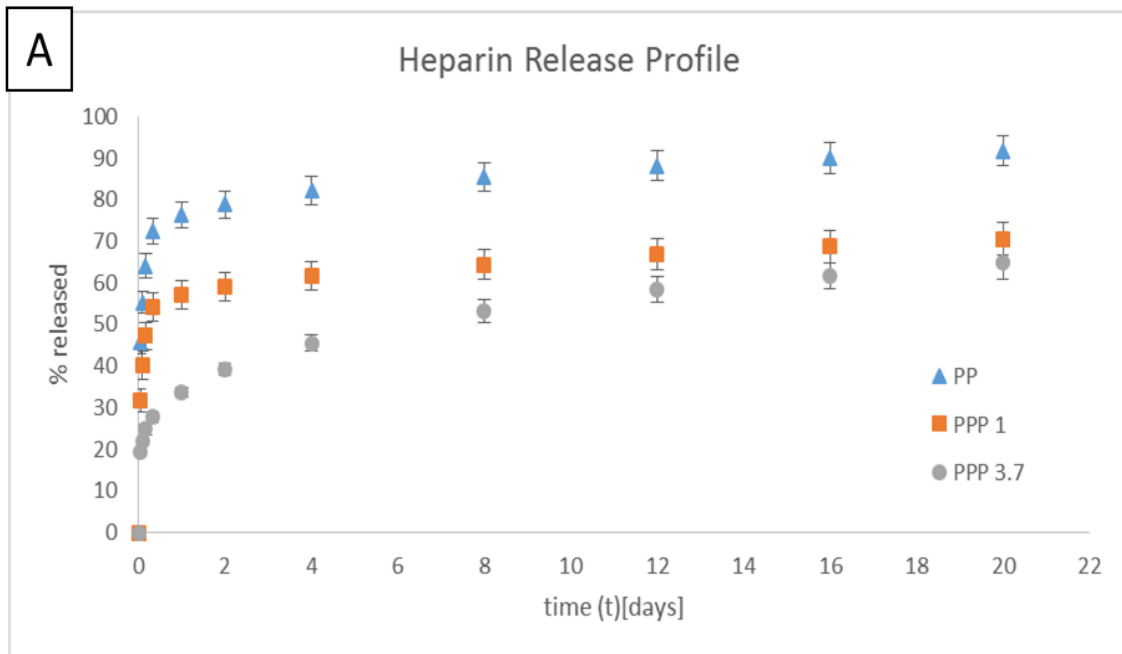


Figure 6. Release profiles of PP, PPP 1 & PPP 3.7 yarns over 20 days (A) and zoomed in profile over first 8 hours (B)

5.5 Immobilized Heparin Therapeutic Activity

The activated partial thromboplastin time (APTT) is a medical test that is used to monitor the effects of heparin on blood [43]. This test was used to test the therapeutic effect of the immobilized heparin. Heparin inhibits factors X and thrombin, while activating anti-thrombin. The calcium chloride is added to activate the coagulation cascade. A 0.1 μg heparin sample was used as standard, and the time for each sample to form a gel-like ‘clot’ was recorded. The results reflected the expected outcome, with the yarns with higher concentrations of immobilized heparin yield higher clotting times. By comparing the clotting time of 0.1 μg to the clotting times of the yarn samples, it can be broken down to follow the release rates of heparin on a per milligram basis.

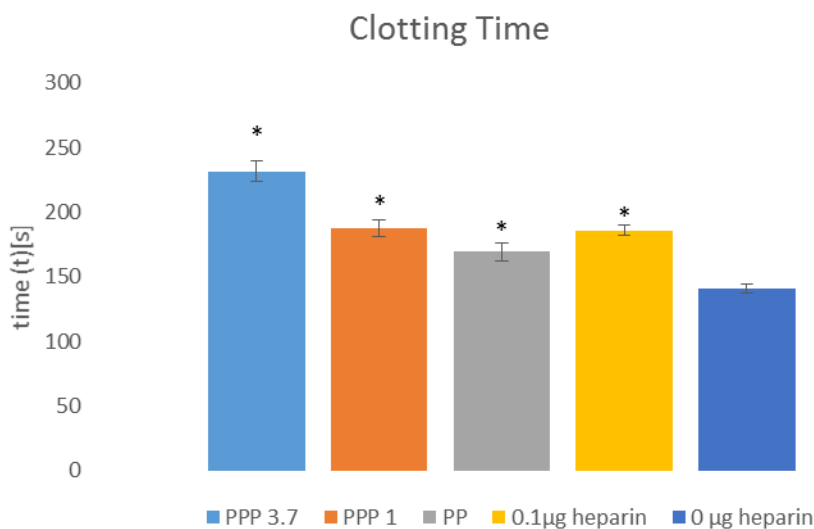


Figure 7. Clotting times of each type of heparin-immobilized yarn $*p < 0.05$ compared to 0 μg heparin solution

Chapter 6

Conclusion and Future Studies

6.1 Conclusion

The goal of this project was to explore the feasibility of a heparin immobilized electrospun yarn as an absorbable suture, specifically for vascular applications. Since the electrospinning process involved a novel polymer (PgP) that was difficult to electrospin, optimizing the electrospinning conditions and polymer blends enabled for uniform fiber formation. The customized collector/twisting device successfully twisted the aligned fiber mass into smooth yarns with little to no surface defects confirmed with SEM imaging.

The project was developed around the application of the PgP polymer to improve heparin loading efficiency and release kinetics of yarns in comparison to non-PgP yarns by taking advantage of the electrostatic attraction between the heparin and PEI in PgP. This goal was accomplished through heparin loading and release studies, showing increased heparin loading amounts in yarns with increased PEI presence. The release profiles also demonstrated a slower, more sustained release of heparin from the yarns with the higher PEI concentrations. To ensure the immobilized heparin was still therapeutically active, an APPT test was performed to measure the clotting times for each sample. Further success was shown with increased clotting times for fibers loaded with more heparin.

The mechanical testing of the fibers was not as successful as the studies prior. All of the fibers tested fell well below the minimum strength requirements for synthetic absorbable sutures of the same size. However, there are several post spinning treatments

and coatings that can be applied to greatly improve the mechanical properties. While some alternative polymers were tested with PgP already in preliminary studies, there still remains other options to optimize the yarn strength.

6.2 Limitations and Future Studies

While the loading and release data is promising, the mechanical properties need to significantly improve for the yarn to be feasible as a surgical suture. In order to achieve this, either a pivot in the project direction needs to be taken where the PgP-heparin loaded fibers are used for an alternative application, or a major processing parameter needs to be changed such as the yarn fabrication method or the polymer solution combination. Incorporating multiple drugs into the yarns for a combinatorial approach is another option to consider for the current state of the project.

References

- [1] K. D. Kochanek, J. Xu, S. L. Murphy, A. M. Minino, and H.-C. Kung, “National Vital Statistics Reports Deaths : Final Data for 2009,” *Natl. Cent. Heal. Stat.*, vol. 60, no. 3, pp. 1–117, 2012.
- [2] C. D. Fryar, T.-C. Chen, and X. Li, “Prevalence of uncontrolled risk factors for cardiovascular disease: United States, 1999-2010.,” *NCHS Data Brief*, no. 103, pp. 1–8, 2012.
- [3] Y. Feng, J. Yang, H. Huang, S. P. Kennedy, T. G. Turi, J. F. Thompson, P. Libby, and R. T. Lee, “Human Vascular Smooth Muscle Cells,” pp. 1118–1123, 1999.
- [4] T. L. Chung, D. W. Pumplun, L. H. Holton, J. a Taylor, E. D. Rodriguez, and R. P. Silverman, “Prevention of microsurgical anastomotic thrombosis using aspirin, heparin, and the glycoprotein IIb/IIIa inhibitor tirofiban.,” *Plast. Reconstr. Surg.*, vol. 120, no. 5, pp. 1281–1288, 2007.
- [5] a. G. Kanani and S. H. Bahrami, “Review on Electrospun Nanofibres Scaffold and Biomedical Applications,” *Trends Biomater. Artif. Organs*, pp. 93–115, 2010.
- [6] S. M. Shridharani, M. K. Folstein, T. L. Chung, and R. P. Silverman, “Prevention of Microsurgical Thrombosis,” *Curr. Concepts Plast. Surg.*, pp. 257–264, 2012.
- [7] C. C. Chu, “Textile-Based Biomaterials for Surgical Applications,” *New York*, 2002.
- [8] M. Scott Taylor and S. W. Shalaby, *Sutures*, Third Edit., no. 2007. Elsevier, 2013.
- [9] J. C. Kim, Y. K. Lee, B. S. Lim, S. H. Rhee, and H. C. Yang, “Comparison of tensile and knot security properties of surgical sutures,” *J. Mater. Sci. Mater. Med.*, vol. 18, no. 12, pp. 2363–2369, 2007.
- [10] “Ethicon Wound Closure Manual,” 2007.
- [11] S. Agarwal, J. H. Wendorff, and A. Greiner, “Use of electrospinning technique for biomedical applications,” *Polymer (Guildf)*, vol. 49, no. 26, pp. 5603–5621, 2008.
- [12] N. Bhardwaj and S. C. Kundu, “Electrospinning: A fascinating fiber fabrication technique,” *Biotechnol. Adv.*, vol. 28, no. 3, pp. 325–347, 2010.
- [13] T. J. Sill and H. A. von Recum, “Electrospinning: Applications in drug delivery and tissue engineering,” *Biomaterials*, vol. 29, no. 13, pp. 1989–2006, 2008.
- [14] E. Luong-Van, L. Grøndahl, K. N. Chua, K. W. Leong, V. Nurcombe, and S. M. Cool, “Controlled release of heparin from poly(ϵ -caprolactone) electrospun

- fibers,” *Biomaterials*, vol. 27, pp. 2042–2050, 2006.
- [15] S. Murugesan, J. Xie, and R. J. Linhardt, “Immobilization of heparin: approaches and applications,” *Curr. Top. Med. Chem.*, vol. 8, no. 2, pp. 80–100, 2008.
- [16] J. R. Sindermann and K. L. March, “Heparin responsiveness in vitro as a prognostic tool for vascular graft stenosis: a tale of two cell types?,” *Circulation*, vol. 97, no. 25, pp. 2486–2490, 1998.
- [17] Y. Su, X. Li, Y. Liu, Q. Su, M. L. W. Qiang, and X. Mo, “Encapsulation and Controlled Release of Heparin from Electrospun Poly(L-Lactide-co-epsilon-Caprolactone) Nanofibers,” *J. Biomater. Sci. Polym. Ed.*, vol. 22, pp. 165–177, 2010.
- [18] C. L. He, Z. M. Huang, and X. J. Han, “Fabrication of drug-loaded electrospun aligned fibrous threads for suture applications,” *J. Biomed. Mater. Res. - Part A*, vol. 89, no. 1, pp. 80–95, 2009.
- [19] W. Hu, Z.-M. Huang, and X.-Y. Liu, “Development of braided drug-loaded nanofiber sutures,” *Nanotechnology*, vol. 21, no. 31, p. 315104, 2010.
- [20] C. B. Weldon, J. H. Tsui, S. A. Shankarappa, V. T. Nguyen, M. Ma, D. G. Anderson, and D. S. Kohane, “Electrospun drug-eluting sutures for local anesthesia,” *J. Control. Release*, vol. 161, no. 3, pp. 903–909, 2012.
- [21] J. E. Lee, S. Park, M. Park, M. H. Kim, C. G. Park, S. H. Lee, S. Y. Choi, B. H. Kim, H. J. Park, J. H. Park, C. Y. Heo, and Y. Bin Choy, “Surgical suture assembled with polymeric drug-delivery sheet for sustained, local pain relief,” *Acta Biomater.*, vol. 9, no. 9, pp. 8318–8327, 2013.
- [22] D. H. Lee, T. Y. Kwon, K. H. Kim, S. T. Kwon, D. H. Cho, S. H. Jang, J. S. Son, and K. B. Lee, “Anti-inflammatory drug releasing absorbable surgical sutures using poly(lactic-co-glycolic acid) particle carriers,” *Polym. Bull.*, vol. 71, no. 8, pp. 1933–1946, 2014.
- [23] J. Zeng, X. Xu, X. Chen, Q. Liang, X. Bian, L. Yang, and X. Jing, “Biodegradable electrospun fibers for drug delivery,” *J. Control. Release*, vol. 92, no. 3, pp. 227–231, Oct. 2003.
- [24] D.-G. Yu, “Electrospun nanofiber-based drug delivery systems,” *Health (Irvine. Calif.)*, vol. 01, no. 02, pp. 67–75, 2009.
- [25] C.-C. Tsai, P. Mikes, T. Andrukh, E. White, D. Monaenkova, O. Burtovyy, R. Burtovyy, B. Rubin, D. Lukas, I. Luzinov, J. R. Owens, and K. G. Kornev, “Nanoporous artificial proboscis for probing minute amount of liquids,” *Nanoscale*, vol. 3, no. 11, p. 4685, 2011.

- [26] R. I. W. Osmond, W. C. Kett, S. E. Skett, and D. R. Coombe, "Protein-heparin interactions measured by BIAcore 2000 are affected by the method of heparin immobilization," *Anal. Biochem.*, vol. 310, no. 2, pp. 199–207, 2002.
- [27] "Carbodiimide Crosslinker Chemistry," *ThermoFisher*. .
- [28] S. E. Naleway, W. Lear, J. J. Kruzic, and C. B. Maughan, "Mechanical properties of suture materials in general and cutaneous surgery," *J. Biomed. Mater. Res. - Part B Appl. Biomater.*, vol. 103, no. 4, pp. 735–742, 2015.
- [29] M. Y. Kariduraganavar, A. A. Kittur, and R. R. Kamble, *Polymer Synthesis and Processing*, 1st ed. Elsevier Inc., 2014.
- [30] L. S. Nair and C. T. Laurencin, "Biodegradable polymers as biomaterials," *Prog. Polym. Sci.*, vol. 32, no. 8–9, pp. 762–798, 2007.
- [31] D. Liang, B. S. Hsiao, and B. Chu, "Functional electrospun nanofibrous scaffolds for biomedical applications," *Adv. Drug Deliv. Rev.*, vol. 59, no. 14, pp. 1392–1412, 2007.
- [32] Y. Z. Zhang, B. Su, S. Ramakrishna, and C. T. Lim, "Chitosan nanofibers from an easily electrospinnable UHMWPEO-doped chitosan solution system," *Biomacromolecules*, vol. 9, no. 1, pp. 136–141, 2008.
- [33] N. Bhattarai, D. Edmondson, O. Veiseh, F. A. Matsen, and M. Zhang, "Electrospun chitosan-based nanofibers and their cellular compatibility," *Biomaterials*, vol. 26, no. 31, pp. 6176–6184, 2005.
- [34] L. Zhao, C. He, Y. Gao, L. Cen, L. Cui, and Y. Cao, "Preparation and cytocompatibility of PLGA scaffolds with controllable fiber morphology and diameter using electrospinning method," *J. Biomed. Mater. Res. - Part B Appl. Biomater.*, vol. 87, no. 1, pp. 26–34, 2008.
- [35] F. Haghghat and S. A. H. Ravandi, "Mechanical properties and in vitro degradation of PLGA suture manufactured via electrospinning," *Fibers Polym.*, vol. 15, no. 1, pp. 71–77, 2014.
- [36] X. Chen, J. Wang, Q. An, D. Li, P. Liu, W. Zhu, and X. Mo, "Electrospun poly(l-lactic acid-co- ϵ -caprolactone) fibers loaded with heparin and vascular endothelial growth factor to improve blood compatibility and endothelial progenitor cell proliferation," *Colloids Surfaces B Biointerfaces*, vol. 128, pp. 106–114, 2015.
- [37] B. Azimi, P. Nourpanah, M. Rabiee, and S. Arbab, "Poly (lactide -co- glycolide) Fiber : An Overview," *J. Eng. Fiber. Fabr.*, vol. 9, no. 1, 2014.
- [38] L. Tian, T. Yan, and Z. Pan, "Fabrication of continuous electrospun nanofiber yarns with direct 3D processability by plying and twisting," *J. Mater. Sci.*, vol. 50,

no. 21, pp. 7137–7148, 2015.

- [39] M. Parthasarathy and S. Sethuraman, *Hierarchical Characterization of Biomedical Polymers*, 1st ed. Elsevier Inc., 2014.
- [40] T. Schneider, B. Kohl, T. Sauter, K. Kratz, A. Lendlein, W. Ertel, and G. Schulze-Tanzil, “Influence of fiber orientation in electrospun polymer scaffolds on viability, adhesion and differentiation of articular chondrocytes,” *Clin. Hemorheol. Microcirc.*, vol. 52, no. 2–4, pp. 325–336, 2012.
- [41] T. Schmitz-rixen, M. Storck, H. Erasmi, P. Schmiegelow, and S. Horsch, “Vascular Anastomoses.”
- [42] a W. Clowes and M. M. Clowes, “Kinetics of cellular proliferation after arterial injury. IV. Heparin inhibits rat smooth muscle mitogenesis and migration.,” *Circ. Res.*, vol. 58, no. 6, pp. 839–45, 1986.
- [43] G. H. Guyatt, E. A. Akl, M. Crowther, D. D. Gutterman, and H. J. Sch??nemann, “Executive summary: Antithrombotic therapy and prevention of thrombosis, 9th ed: American College of Chest Physicians evidence-based clinical practice guidelines,” *Chest*, vol. 141, no. 2 SUPPL. 2012.